NASA Technical Memorandum 86704

Bifurcation Theory Applied to Aircraft Motions

W.H. Hui and M. Tobak

March 1985

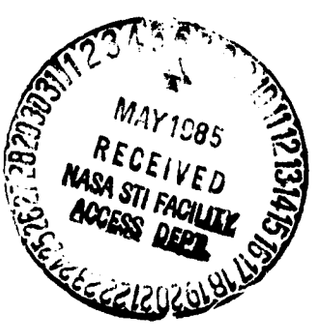

National Aeronautics and
Space Administration

NASA Technical Memorandum 86704

Bifurcation Theory Applied to Aircraft Motions

W. H. Hui, University of Waterloo, Waterloo, Ontario, Canada
M. Tobak, Ames Research Center, Moffett Field, California

March 1985

National Aeronautics and
Space Administration

Ames Research Center
Moffett Field, California 94035

BIFURCATION THEORY APPLIED TO AIRCRAFT MOTIONS

W. H. Hui
Professor of Applied Mathematics and Mechanical Engineering
University of Waterloo, Waterloo, Ontario, Canada N2L 3G1

Murray Tobak
Research Scientist
NASA Ames Research Center, Moffett Field, California 94035, U.S.A.

SUMMARY

Bifurcation theory is used to analyze the nonlinear dynamic stability characteristics of single-degree-of-freedom motions of an aircraft or a flap about a trim position. The bifurcation theory analysis reveals that when the bifurcation parameter, e.g., the angle of attack, is increased beyond a critical value at which the aerodynamic damping vanishes, a new solution representing finite-amplitude periodic motion bifurcates from the previously stable steady motion. The sign of a simple criterion, cast in terms of aerodynamic properties, determines whether the bifurcating solution is stable (supercritical) or unstable (subcritical). For the pitching motion of a flat-plate airfoil flying at supersonic/hypersonic speed, and for oscillation of a flap at transonic speed, the bifurcation is subcritical, implying either that exchanges of stability between steady and periodic motion are accompanied by hysteresis phenomena, or that potentially large aperiodic departures from steady motion may develop. On the other hand, for the rolling oscillation of a slender delta wing in subsonic flight (wing rock), the bifurcation is found to be supercritical. This and the predicted amplitude of the bifurcation periodic motion are in good agreement with experiments.

1. INTRODUCTION

Problems of aerodynamic stability of aircraft flying at small angles of attack have been studied extensively. With increasing angles of attack the problems become more complicated and typically involve nonlinear phenomena such as coupling between modes, amplitude and frequency effects, and hysteresis. The need for investigating stability characteristics at high angles of attack was clearly demonstrated by Orlik-Rückemann (Ref. 1) in his survey paper which deals largely with experiments.

On the theoretical side, much of an extensive body of work is based on the linear theory, in which the unsteady flow is regarded as a small perturbation of some known steady flow (possibly nonlinear in, e.g., the angle of attack) that prevails under certain flight conditions. The question of the validity and limitations of such a linearized perturbation theory is of fundamental importance. Yet, it has rarely been investigated. One may argue that, in principle, it should be possible to advance to higher and higher angles of attack α by a series of linear perturbations since the solution at each step should include a steady-state part which, when added to the previous steady-state solution, would provide the starting point for the next perturbation. This may well be true provided that at each step the steady motion is both statically and dynamically stable, and that the actual disturbances, e.g., the amplitude of oscillation, remain small. However, when the angle of attack exceeds a certain critical value α_{cr} at which the steady motion is no longer stable, the linear theory predicts an exponential growth of the perturbation with time and, therefore, must cease to be valid after finite time. The motion of the aircraft under these conditions can only be studied by means of a nonlinear theory.

In this paper we investigate three types of problems in which a steady motion becomes unstable. Padfield (Ref. 2) studied a similar class of problems using the method of multiple scales, which is valid only for weakly nonlinear oscillations. We shall study the problem using bifurcation theory. This allows us to draw on recent mathematical developments (see Ref. 3) that are particularly well-suited to investigating fundamental questions in linear and nonlinear stability theory. A numerical scheme based on bifurcation theory was proposed earlier (Ref. 4) for analyzing aircraft dynamic stability in a general framework. More recent work by Guicheteau (Ref. 5) demonstrates the considerable potential of bifurcation theory in flight dynamics studies, particularly toward establishing a method for the design of flight control systems to ensure protection against loss of control. While acknowledging the importance of the aerodynamic model in determining aircraft stability characteristics, neither study contains an adequate assessment of the model requirements. The treatment of unsteady flow effects receives no attention. In contrast, we shall focus on just this aspect of the motion analysis.

We shall restrict this study to the single-degree-of-freedom motions, e.g., pitching or rolling, of an aircraft about its trimmed flight condition. This enables us to analyze motions for which complete aerodynamic information (exact analytical or numerical solutions) is available for certain shapes. The information is obtained from solutions of the unsteady inviscid flow equations (Refs. 6-12) or from results of experiments (Ref. 13). In this way it is possible to establish a form revealing a precise analytical relationship between the basic aerodynamic coefficients and the characteristics of the motion.

Specifically we shall consider the following three examples:

A. Pitching supersonic/hypersonic airfoil in rectilinear flow (Fig. 1);

B. Flap oscillations in transonic flow (Fig. 2);

C. Wing rock of a slender delta wing in subsonic flow (Fig. 3).

2. MATHEMATICAL FORMULATION

Let the aircraft or flap be in level, trimmed flight until time $t = 0$ when it is perturbed from its trim position. During the subsequent motion the center of gravity continues to follow a rectilinear path at constant velocity V_∞. For a single-degree-of-freedom oscillatory motion, the equation of motion is

$$I \frac{d^2\xi}{dt^2} = G(t;\lambda) \tag{1}$$

where $\xi(t)$ is the instantaneous angle-of-attack perturbation in example A, flap-angle perturbation in example B, and roll angle in example C; I is the appropriate moment of inertia; and $G(t)$ is the corresponding instantaneous perturbation moment of the aerodynamic forces.

In Eq. (1), λ represents a set of parameters defining steady flight at the trim condition. Flight Mach number M_∞, ratio of specific heats γ, and trim angle of attack α_m are included in these parameters. We shall consider λ to be the trim angle of attack α_m in examples A and C, and the mean flap deflection angle δ_m in example B. In other words, all other defining parameters will be held fixed when considering the consequence of varying λ on aircraft motion characteristics. We assume that the moment required to trim the aircraft or flap at λ has been accounted for, so that $G(t;\lambda)$ is a measure of the perturbation moment only.

The instantaneous motion state, $\xi(t)$ and $\dot{\xi}(t)$, and the instantaneous moment $G(t)$ are a result of the interaction of aircraft or flap motion and the unsteady aerodynamic forces from time zero to time t. Consequently, the instantaneous moment $G(t)$ depends not only on the instantaneous motion state, $\xi(t)$ and $\dot{\xi}(t)$, but also on the past motion history from time zero to t. This is to say that $G(t)$ is a functional of $\xi(t_1)$, $(0 \le t_1 \le t)$ as described in Ref. 14. Thus

$$G(t) = G\Big[\xi(t_1)\Big]_0^t \tag{2}$$

For motions for which $\xi(t_1)$ is analytic, the functional is equivalent to a function of an infinite set of variables,

$$G(t) = G\Big[\xi(t_1)\Big]_0^t$$

$$= G\left(\xi(t),\ \dot{\xi}(t),\ \ddot{\xi}(t),\ldots,\ \frac{d^n\xi(t)}{dt^n},\ \ldots\right) \tag{3}$$

For most problems encountered in the study of dynamic stability, the motion is slow although its amplitude may be finite or large. Under these conditions $\ddot{\xi}(t)$, $\dddot{\xi}(t)$, ... in Eq. (3) may be neglected and, as a first approximation

$$G(t) = G(\xi(t),\dot{\xi}(t)) \tag{4}$$

We further assume that G is an analytic function of ξ and $\dot{\xi}$. Expanding Eq. (4) as a Taylor series, we neglect terms of $O(\dot{\xi}^2)$ and higher for slow motions, and after reintroducing the parameter λ,

$$G(t;\lambda) = G_0(\xi(t);\lambda) + \frac{\dot{\xi}(t)\ell}{V_\infty} G_1(\xi(t);\lambda) \tag{5}$$

where ℓ is a characteristic length and

$$G_0(0;\lambda) = 0 \tag{6}$$

as required at the trim condition. The form of the instantaneous moment $G(t;\lambda)$ in Eq. (5) is consistent with the exact analytic solution for the pitching moment in example A (Ref. 10), the numerical solution for the hinge moment in example B (Ref. 12), and the experimentally derived empirical formula for the rolling moment in example C (Ref. 13).

In summary, the single-degree-of-freedom motions considered in this paper will be based on the following mathematical problem

$$I\frac{d^2\xi}{dt^2} = G_0(\xi;\lambda) + \frac{\dot{\xi}\ell}{V_\infty}G_1(\xi;\lambda) = G(\xi,\dot{\xi};\lambda) \tag{7a}$$

$$\xi(0) = \hat{\xi}_0 \tag{7b}$$

$$\dot{\xi}(0) = \hat{\xi}_1 \tag{7c}$$

The functions $G_0(\xi;\lambda)$ and $G_1(\xi;\lambda)$ are generally nonlinear in ξ and have to be determined from the study of unsteady aerodynamics, either theoretically or experimentally. Evidently G_0 is related to the restoring moment and G_1 is related to the damping moment.

In many situations, it is known that when the parameter λ reaches some critical value λ_{cr}, the aerodynamic damping G_1 vanishes and steady flight at the trim condition λ_{cr} loses its stability. We use bifurcation theory to determine the motion characteristics of an aircraft or flap whose trim condition is near or beyond λ_{cr}.

3. BIFURCATION THEORY

We introduce the dimensionless time $\tau = V_\infty t/\ell$, where ℓ is a characteristic length, equal to the chord length of the airfoil in example A, the chord length of the forebody plus flap in example B, and the chord length of the wing in example C. Hereafter we use $(')$ to denote $d/d\tau$. We further let

$$\begin{aligned} F(\xi,\dot{\xi};\lambda) &= G(\xi,\dot{\xi};\lambda)/(I\,V_\infty^2/\ell^2) \\ &= F_0(\xi;\lambda) + \dot{\xi}F_1(\xi;\lambda) \end{aligned} \tag{8}$$

Then Eq. (7a) may be written

$$\frac{d\xi}{d\tau} = \dot{\xi} \tag{9a}$$

$$\frac{d\dot{\xi}}{d\tau} = F(\xi,\dot{\xi};\lambda) \tag{9b}$$

An expansion of $F(\xi,\dot{\xi};\lambda)$ in a Taylor series in ξ and $\dot{\xi}$ and a change of notation $u_1 = \xi$, $u_2 = \dot{\xi}$ yield for Eqs. (9)

$$\dot{u}_i = A_{ij}(\lambda)u_j + B_{ijk}(\lambda)u_ju_k + C_{ijk\ell}(\lambda)u_ju_ku_\ell + O(|\vec{u}|^4), \quad (i = 1,2) \tag{10}$$

where

$$A = \begin{bmatrix} 0 & 1 \\ -S(\lambda) & -D(\lambda) \end{bmatrix} \tag{11a}$$

$$S(\lambda) = -F_0'(0;\lambda), \quad D(\lambda) = -F_1(0;\lambda) \tag{11b}$$

$$B_{1jk} = 0, \quad B_{2jk} = \frac{1}{2!}\left.\frac{\partial^2 F}{\partial u_j \partial u_k}\right|_{\vec{u}=0} \tag{11c}$$

and

$$C_{1jk\ell} = 0, \quad C_{2jk\ell} = \frac{1}{3!}\left.\frac{\partial^3 F}{\partial u_j \partial u_k \partial u_\ell}\right|_{\vec{u}=0} \tag{11d}$$

(Although Eqs. (9) have been derived on the assumption of slow oscillations, subsequent bifurcation analysis of Eq. (9) will hold for general $F(\xi,\dot{\xi};\lambda)$, i.e., as if no restriction had been placed on the magnitude of $\dot{\xi}$.)

In Eqs. (11), the tensors B and C represent the effects of finite amplitude to the second and third order. The following symmetry properties hold:

$$B_{2jk} = B_{2kj} \tag{12a}$$

$$C_{2jk\ell} = C_{2j\ell k} = C_{2k\ell j} = C_{2\ell jk} = C_{2\ell kj} \tag{12b}$$

On the basis of Eq. (10), we discuss the linear and nonlinear stability of the motion.

3.1 Linear Stability Theory

The stability of steady motion at the trim condition λ to infinitesimal disturbances is determined by the nature of the eigenvalues of the matrix A. They are

$$\eta_{1,2}(\lambda) = \frac{1}{2}\left[-D(\lambda) \pm \sqrt{D^2(\lambda) - 4S(\lambda)}\right] \tag{13}$$

Case I: $S(\lambda) < 0$. In this case, $\eta_1 > 0$, $\eta_2 < 0$. The steady motion at this condition λ is always unstable.

Case II: $S(\lambda) > 0$.

IIa: $D(\lambda) < 0$. In this case, $\mathrm{Re}(\eta_{1,2}) > 0$ and the steady motion at λ is unstable.

IIb: $D(\lambda) > 0$. In this case, $\mathrm{Re}(\eta_{1,2}) < 0$ and the steady motion at λ is stable.

Only in Case IIb, when both stiffness derivative $S(\lambda)$ and damping derivative $D(\lambda)$ are positive, is the steady motion at the trim condition λ stable to infinitesimal disturbances. In fact, stability theory (Ref. 3) can be used to show that stability of the steady motion in this case is assured if and only if the disturbance is sufficiently small.

When linear theory predicts growth of the disturbance amplitude, growth is exponential and the linear theory is no longer valid when the amplitude becomes large after a finite time. What happens to a motion with growth of disturbances predicted from linear theory cannot be predicted by using only the linear theory. To determine the ultimate state of motion, the full nonlinear inertial equation (or a suitable approximation of it, such as Eq. 10) must be used. Of particular interest is the dynamic stability boundary $\lambda = \lambda_{cr}$, where $S(\lambda_{cr}) > 0$ and $D(\lambda_{cr}) = 0$. The stability characteristics near this boundary will be studied presently.

3.2 Hopf Bifurcation Theory

At the dynamic stability boundary $\lambda = \lambda_{cr}$, we have $S(\lambda_{cr}) > 0$; hence,

$$\eta_{1,2}(\lambda_{cr}) = \pm i\sqrt{S(\lambda_{cr})} = \pm i\omega_0 \tag{14}$$

The existence of purely imaginary eigenvalues of the matrix A at $\lambda = \lambda_{cr}$ is the characteristic sign of a Hopf bifurcation (Refs. 3 and 15), signaling a changeover from stable steady motion to periodic motion. On crossing $\lambda = \lambda_{cr}$, the steady motion that had been stable for $\lambda < \lambda_{cr}$ becomes unstable to disturbances, resulting (after a transient motion has died away) in the existence of a new motion, which (if it is stable) is periodic. In the vicinity of $\lambda = \lambda_{cr}$, the circular frequency of the periodic motion is nearly equal to ω_0. We call the new solution of the equation of motion a bifurcation solution. In this section we shall determine its character and a criterion for its stability.

For λ slightly larger than λ_{cr}, the eigenvalues of the matrix A are

$$\eta_{1,2} = -\frac{1}{2}D(\lambda) \pm i\Omega(\lambda) \tag{15}$$

where

$$\Omega(\lambda) = \sqrt{S(\lambda) - D^2(\lambda)/4} \tag{16}$$

We shall assume that

$$D'(\lambda_{cr}) < 0 \tag{17}$$

which is the usual case in applications. (The case $D'(\lambda_{cr}) > 0$ can be treated in exactly the same way.) The normalized eigenvector $\xi(\lambda)$ associated with the eigenvalue $\eta(\lambda)$ is

$$\vec{\xi}(\lambda) = \begin{bmatrix} \xi_1(\lambda) \\ \xi_2(\lambda) \end{bmatrix} = \frac{1-i}{2\sqrt{Q(\lambda)}} \begin{bmatrix} 1 \\ \eta(\lambda) \end{bmatrix} \tag{18}$$

whereas the adjoint eigenvector $\vec{\xi}^*(\lambda)$ with eigenvalue $\bar{\eta}(\lambda)$, which is the complex conjugate of $\eta(\lambda)$, is

$$\vec{\xi}^*(\lambda) = \begin{bmatrix} \xi_1^*(\lambda) \\ \xi_2^*(\lambda) \end{bmatrix} = \frac{1+i}{2\sqrt{Q(\lambda)}} \begin{bmatrix} \bar{\eta}(\lambda) + D(\lambda) \\ 1 \end{bmatrix} \tag{19}$$

A. Hopf Bifurcation. The bifurcation solution $\vec{u}(\tau,\lambda)$ may be written as

$$\vec{u} = a(\tau)\vec{\xi} + \bar{a}(\tau)\bar{\vec{\xi}} \tag{20}$$

Following Iooss and Joseph (Ref. 3, p. 125), we get

$$\left.\begin{aligned} a &= \varepsilon b_1(s) + \varepsilon^2 b_2(s) + \varepsilon^3 b_3(s) + O(\varepsilon^4) \\ s &= [\omega_0 + \varepsilon^2\omega_2 + O(\varepsilon^4)]\tau \\ \lambda &= \lambda_{cr} + \varepsilon^2\lambda_2 + O(\varepsilon^4) \end{aligned}\right\} \tag{21}$$

where, for brevity, we omit the lengthy solutions for ξ_i, b_n, ω_2, and λ_2 (Ref. 11). The solution is periodic in τ with circular frequency equal to $\omega_0 + \varepsilon^2\omega_2 + O(\varepsilon^4)$.

B. Stability of the Bifurcation Periodic Solution. According to Floquet theory (Ref. 3), the stability of the bifurcation periodic solution Eq. (21) is determined by the sign of an index μ. To $O(\varepsilon^4)$, μ has the form

$$\mu = D'(\lambda_{cr})\lambda_2\varepsilon^2 + O(\varepsilon^4) \tag{22}$$

The bifurcation periodic solution is stable if $\mu < 0$ and unstable if $\mu > 0$. Since we have assumed $D'(\lambda_{cr}) < 0$, stability depends on the sign of λ_2, with $\lambda_2 > 0$ denoting stability and $\lambda_2 < 0$ instability. It remains to cast λ_2 in more recognizable terms. Considerable manipulation yields

$$\mu = \frac{\varepsilon^2}{4\omega_0^3}\left[\left(\frac{\partial^2 F}{\partial u_1^2} + \omega_0^2\frac{\partial^2 F}{\partial u_2^2}\right)\frac{\partial^2 F}{\partial u_1 \partial u_2} + \omega_0^2\left(\frac{\partial^3 F}{\partial u_1^2 \partial u_2} + \omega_0^2\frac{\partial^3 F}{\partial u_2^3}\right)\right]_{\substack{\vec{u}=0 \\ \lambda=\lambda_{cr}}} \tag{23}$$

in terms of $F(u_1,u_2;\lambda)$. From Eq. (8) we see that the function F is directly related to the moment $G(\xi,\dot{\xi};\lambda)$ acting on the aircraft or flap which is performing a finite-amplitude oscillation ξ around the trim position λ. Equation (23) demonstrates that the stability of periodic motion near the dynamic stability boundary λ_{cr} is determined by the behavior of the aerodynamic response $G(\xi,\dot{\xi};\lambda)$ in that vicinity.

With the assumption of slow oscillations under which the form of Eq. (5) was derived (terms of $O(\dot{\xi}^2,\ddot{\xi})$ neglected), we may substitute Eq. (5) with Eq. (8) into Eq. (23) to get

$$\mu = \frac{\varepsilon^2}{4\omega_0^3}\left(F_0''F_1' + \omega_0^2 F_1''\right)_{\substack{\xi=0 \\ \lambda=\lambda_{cr}}} \tag{24}$$

Since from Eqs. (14) and (11b)

$$\omega_0 = \sqrt{S(\lambda_{cr})} = \sqrt{-F_0'(0;\lambda_{cr})} \tag{25}$$

Eq. (24) becomes, after using Eq. (8),

$$\mu = -\frac{\varepsilon^2\omega_0}{4}\left[\frac{d}{d\xi}\left(\frac{F_1'(\xi;\lambda_{cr})}{F_0'(\xi;\lambda_{cr})}\right)\right]_{\xi=0} \tag{26a}$$

or

$$\mu = -\frac{\varepsilon^2\omega_0}{4}\left[\frac{d}{d\xi}\left(\frac{G_1'(\xi;\lambda_{cr})}{G_0'(\xi;\lambda_{cr})}\right)\right]_{\xi=0} \tag{26b}$$

Using Eq. (10) we get

$$\mu = \frac{\epsilon^2 \omega_0}{2} \frac{C_{2112}(\lambda_{cr})}{S(\lambda_{cr})} \tag{26a}$$

We have thus established the following criterion: bifurcation periodic motion is stable or unstable according to

$$\mu < 0 \quad \text{or} \quad \mu > 0 \tag{27a}$$

or alternatively, since $S(\lambda_{cr}) > 0$, according to

$$C_{2112}(\lambda_{cr}) < 0 \quad \text{or} \quad C_{2112}(\lambda_{cr}) > 0 \tag{27b}$$

The two possibilities are well illustrated in the form of bifurcation diagrams as shown in Figs. 4a and 4b.

In a bifurcation diagram, the abscissa represents the bifurcation parameter λ, while the ordinate is a parameter characteristic of the bifurcation solution alone. In this case it is ϵ, a measure of the amplitude of the bifurcation periodic solution. Stable solutions are indicated by solid lines and unstable solutions are indicated by dashed lines. Thus over the range of the bifurcation parameter $\lambda < \lambda_{cr}$ where the steady-state motion is stable, ϵ is zero, and the stable steady motion is represented along the abscissa by a solid line. The steady motion becomes unstable for all values of $\lambda > \lambda_{cr}$ as the dashed line along the abscissa indicates. Periodic solutions bifurcate from $\lambda = \lambda_{cr}$, either supercritically or subcritically.

When $C_{2112}(\lambda_{cr}) < 0$, hence $\mu < 0$ (implying $\lambda_2 > 0$), the bifurcation is called supercritical and its characteristic form is shown in Fig. 4a. In this case, stable periodic solutions (solid curves in Fig. 4a) exist for values of $\lambda > \lambda_{cr}$. The amplitude of the periodic solution at a given value of $\lambda - \lambda_{cr}$ is proportional to ϵ, hence is vanishingly small when $\lambda - \lambda_{cr}$ is small, varying essentially as $(\lambda - \lambda_{cr})^{1/2}$.

When $C_{2112}(\lambda_{cr}) > 0$ hence $\mu > 0$ (implying $\lambda_2 < 0$), the bifurcation is called subcritical and its characteristic form is shown in Fig. 4b. In this case, periodic solutions exist for values of $\lambda < \lambda_{cr}$, but they are unstable (dashed curve in Fig. 4b). The existence of stable periodic solutions for $\lambda > \lambda_{cr}$ depends predominantly on the behavior of the damping $G_1(\xi;\lambda)$ for $\lambda > \lambda_{cr}$. If no stable periodic solutions exist for $\lambda > \lambda_{cr}$, then when λ is increased beyond λ_{cr} the aircraft or flap may undergo an aperiodic motion whose departure from the steady motion at $\lambda = \lambda_{cr}$ is potentially large.

In the more likely event that stable periodic solutions do exist for $\lambda > \lambda_{cr}$, their amplitudes must be finite, and not infinitesimally small, even for small positive values of $\lambda - \lambda_{cr}$. It is likely that this branch of stable periodic solutions will join that of the unstable branch as illustrated in Fig. 4b. In this event, the form of the bifurcation curve for values of $\lambda < \lambda_{cr}$ helps explain the situation where the steady-state motion could be stable to sufficiently small disturbances but become unstable to larger disturbances. For $\lambda < \lambda_{cr}$, Fig. 4b suggests disturbances with small enough amplitudes (lying below curve OB) will die out and the steady motion will remain stable. However, disturbances with amplitudes sufficiently larger than those of the unstable branch may actually grow up to the ultimate motion as $\tau \to \infty$, which will be that of the stable branch of periodic solutions (curve BA in Fig. 4b). Finally, we note that if the motion does attain the stable branch of periodic solutions (say, for $\lambda < \lambda_{cr}$), then hysteresis effects will manifest themselves with further changes in λ. When λ is increased beyond λ_{cr}, motion will continue to be periodic with finite amplitude (point A in Fig. 4b). If λ is now decreased below λ_{cr}, periodic motion will persist, even at values of λ where previously there had been steady motion when λ was being increased. Not until λ is diminished beyond a certain point (point B in Fig. 4b) will the motion return to the steady-state condition (point C in Fig. 4b) that had been experienced when λ was increasing.

4. APPLICATIONS TO AIRCRAFT MOTIONS

In this section we shall apply the theory developed in Secs. 2 and 3 to three different single-degree-of-freedom motions.

4.1 Pitching Motion of Supersonic/Hypersonic Airfoil

We retain the symbol ξ in all three cases to designate the perturbation variable. The other symbols will be replaced as necessary by the parameters relevant to the particular motion.

In the case of pitching oscillation (Fig. 1) of a supersonic/hypersonic airfoil in rectilinear flight, the parameter λ is the trim angle of attack, designated α_m in Fig. 1, measured relative to the horizontal velocity vector. The instantaneous angle of attack is $\alpha(t)$, also measured relative to the horizontal velocity vector, so that the perturbation variable $\xi(t)$ is the inclination $\alpha(t) - \alpha_m$ from the fixed trim angle of attack. The perturbation moment G in this case is the perturbation pitching moment about the center of gravity. Thus,

$$G(t;\lambda) = qS\ell C_m(t;\alpha_m,M_\infty,\gamma,h) \tag{28}$$

where q is the dynamic pressure, and S and ℓ are the reference area and length. The instantaneous pitching-moment coefficient C_m is also a function of the trim angle of attack α_m, the flight Mach number M_∞, the ratio of specific heat γ, and the (dimensionless) pivot axis position h.

For large-amplitude slow oscillations, exact solutions for C_m exist for simple shapes (Refs. 10 and 11), and their form is consistent with Eq. (5), i.e.,

$$C_m(\tau;\alpha_m) = C_{m_0}(\xi(\tau);\alpha_m) + \dot{\xi}C_{m_1}(\xi(\tau);\alpha_m) - C_{m_0}(0;\alpha_m) \tag{29}$$

Moreover, it is shown that (Refs. 10 and 11)

$$C_{m_i}(\xi;\alpha_m) = C_{m_i}(\xi + \alpha_m) , \quad (i = 0, 1) \tag{30}$$

Accordingly

$$\frac{\partial C_{m_i}}{\partial \xi} = \frac{\partial C_{m_i}}{\partial \alpha_m} \qquad (i = 0, 1) \tag{31}$$

and Eq. (26b) reduces to

$$\mu = -\frac{\varepsilon^2\omega_0}{4}\frac{d}{d\alpha_m}\left[\frac{D'(\alpha_m)}{S(\alpha_m)}\right]_{\alpha_m=\alpha_{cr}} \tag{32}$$

where the stiffness derivative $S(\alpha_m)$ and the damping-in-pitch derivative $D(\alpha_m)$ are related to the pitching-moment coefficient C_m by

$$S(\alpha_m) = -C'_{m_0}(\alpha_m) , \qquad D(\alpha_m) = -C_{m_1}(\alpha_m) \tag{33}$$

and

$$D(\alpha_{cr}) = 0 \tag{34}$$

A typical example of the variation of damping derivative $D(\alpha_m)$ versus α_m is shown in Fig. 5 (Ref. 16).

We conclude that when the trim angle of attack α_m is increased beyond a critical value α_{cr} at which the aerodynamic damping vanishes, i.e., $D(\alpha_{cr}) = 0$, the steady motion at α_{cr} loses its stability. A new finite-amplitude periodic motion, called the bifurcation solution, will replace it for values of $\alpha_m \geq \alpha_{cr}$ if it is stable. Stability of the bifurcation solution depends on whether $D'(\alpha_m)/S(\alpha_m)$ is increasing or decreasing on crossing the stability boundary α_{cr}.

By utilizing an approximate relation (Ref. 17)

$$D(\alpha_m) = b[S(\alpha_{cr}) - S(\alpha_m)] , \qquad b > 0$$

in Eq. (32), we get

$$\mu = \frac{\varepsilon^2\omega_0 b}{4}\left[\frac{d^2}{d\alpha_m^2}\ln S(\alpha_m)\right]_{\alpha_m=\alpha_{cr}}$$

For the case of a flat-plate airfoil in supersonic/hypersonic flow, the stiffness and damping-in-pitch derivatives $S(\alpha_m)$ and $D(\alpha_m)$ are known exactly in analytical form (Ref. 7) for values of α_m up to the shock detachment angle. It is shown in Table 1 that $\mu > 0$ for all combinations of M_∞ and h. Thus, the bifurcation is subcritical. The bifurcation periodic solution is therefore unstable, which implies one of two alternatives. The steady motion is either replaced by a finite-amplitude periodic motion accompanied by hysteresis phenomena, or by a potentially large aperiodic motion. In either case the loss of stability of the steady-state motion must be accompanied by a discrete change to a new stable state.

4.2 Flap Oscillation in Transonic Flow

The case of a flap oscillating about a hinge is conceptually similar to that of an airfoil pitching about a pivot axis. In effect, the oscillating flap may be regarded as an airfoil pitching in the nonuniform oncoming stream that results from a uniform free stream passing over the fixed forebody (Fig. 2).

In this case (Fig. 2), $\delta(t)$ is the instantaneous flap deflection angle, measured relative to the undeflected position. The parameter λ here is the fixed mean deflection angle δ_m, also measured from the undeflected position. Thus, $\xi(t)$, the perturbation variable, is the inclination $\delta(t) - \delta_m$ from the fixed mean deflection angle δ_m. The perturbation moment Q is the perturbation hinge moment about the hinge line. Thus

$$Q(t;\lambda) = qS\ell C_h(t;\delta_m,M_\infty,\gamma) \tag{35}$$

where C_h is the instantaneous hinge-moment coefficient. In direct parallel with the oscillating airfoil case of Eq. (29), we assign C_h the form

$$C_h(\tau;\delta_m) = C_{h_0}(\xi(\tau);\delta_m) + \dot{\xi}C_{h_1}(\xi(\tau);\delta_m) - C_{h_0}(0;\delta_m) \tag{36}$$

Equation (36) is consistent with Eq. (5). A similar form was validated in Ref. 12 by comparison with results of large-scale numerical integrations of the coupled inertial/flow field equations.

Equation (5) or Eq. (36) for the hinge-moment coefficient allows calculation of $C_{h_1}(\xi(\tau);\delta_m)$ by linearizing the flow field equations about the steady flow corresponding to fixing the instantaneous deflection angle, $\xi(\tau) + \delta_m$ (see Eq. (39)). Calculation of $C_{h_1}(\xi(\tau);\delta_m)$ from the linearized equations may require less computing time than the nonlinear method used in Ref. 12, yet it is consistent with the level of approximation leading to Eq. (5) or Eq. (36). This simplification of the calculation of $C_{h_1}(\xi(\tau);\delta_m)$ reinforces the main conclusion of Ref. 12 that the cost of computations to determine the flap's motion will be very small if the aerodynamic contribution to the equations of motion is modeled, as compared to the computational cost required to solve the coupled inertial/flow field equations.

It was further established (Ref. 11) that

$$C_{h_i}(\xi;\delta_m) = C_{h_i}(\xi + \delta_m) , \quad (i = 0, 1) \tag{37}$$

which in turn reduces Eq. (26b) to

$$\mu = -\frac{\epsilon^2\omega_0}{4}\left[\frac{d}{d\delta_m}\frac{D'(\delta_m)}{S(\delta_m)}\right]_{\delta_m=\delta_{cr}} \tag{38}$$

where

$$S(\delta_m) = -C'_{h_0}(\delta_m) , \quad D(\delta_m) = -C_{h_1}(\delta_m) , \quad D(\delta_{cr}) = 0 \tag{39}$$

We therefore reach a conclusion regarding the characteristics of the flap oscillation near the mean flap deflection angle δ_{cr} which is directly analogous to that of Sec. 4.1 regarding the characteristics of the airfoil pitching motion in the neighborhood of α_{cr}.

Numerical results from Ref. 12 for $S(\delta_m)$ and $D(\delta_m)$ are reproduced (by means of spline fitting) in Fig. 6. These are results for an NACA 64A010 airfoil at zero mean angle of attack in a transonic stream with $M_\infty = 0.8$ and $\gamma = 1.4$. It is found that

$$\left[\frac{d}{d\delta_m}\frac{D'(\delta_m)}{S(\delta_m)}\right]_{\delta_m=\delta_{cr}} = -59.20 \quad \text{at} \quad \delta_{cr} = 2.7°$$

Hence, the bifurcation is subcritical and the bifurcation periodic solution is unstable. Just as we found for the flat-plate airfoil in supersonic/hypersonic flow, loss of stability of the steady-state transonic flow about the flap at $\delta_m = \delta_{cr}$ implies a <u>discrete</u> change to a new stable state. The new state may be either a finite-amplitude periodic oscillation about δ_m accompanied by hysteresis phenomena, or it may be a potentially large aperiodic departure from the steady state. The fact that $D(\delta_m)$ becomes positive again at $|\delta_m| = 17°$ (Fig. 6(b)) implies that the first of these alternatives will be the preferred one (Ref. 11).

4.3. Wing Rock of Slender Delta Wing in Subsonic Flow

The phenomenon known as "wing rock" of a slender delta wing in subsonic flow has been the subject of intensive investigation by many researchers (Refs. 13, 18-21). It is now well-documented (Refs. 13 and 18) that as the trim angle of attack α_m is raised incrementally, a critical value α_{cr} is reached where roll-damping moment changes from stabilizing to destabilizing. Ericsson (Ref. 21) has shown how the leeside vortices, which appear and grow stronger as α_m is raised, may lag behind a rolling motion of the wing. The pressures they induce may contribute a rolling-moment component proportional to rolling velocity that is destabilizing and eventually becomes large enough to surpass the stabilizing component that had existed

alone at smaller α_m. Consequently, at $\alpha_m \gtrsim \alpha_{cr}$, small disturbances in the flow field excite a growing roll oscillation. Bifurcation theory again can be applied to help determine the ultimate state of the oscillation.

For this case, we take the parameter λ to be the fixed trim angle of attack α_m, while the perturbation variable $\xi(t)$ is the roll deflection angle $\phi(t)$ (Fig. 3), measured from the position of zero roll angle. The perturbation moment G is the rolling moment about the wing longitudinal axis. Thus

$$G(t;\lambda) = qS\ell C_\ell(t;\alpha_m,\Lambda) \tag{40}$$

where, for incompressible flow, the instantaneous rolling-moment coefficient C_ℓ depends on the trim angle of attack α_m and the sweepback angle Λ of the delta wing. Results of experiments (Refs. 13 and 18) and numerical computations (Ref. 19) have shown that, for a given Λ, it is a good approximation to the instantaneous rolling-moment coefficient to take

$$C_\ell = C_{\ell_0}(\xi(\tau);\alpha_m) + \dot{\xi}C_{\ell_1}(\xi(\tau);\alpha_m) \tag{41}$$

which is consistent with Eq. (5).

As an example, for the 80° sweep-back flat delta wing studied in Ref. 18, C_ℓ is approximated by a power series (Ref. 19) which leads to the following equation for the rolling motion

$$\begin{aligned}\ddot{\xi} &= F(\xi,\dot{\xi};\alpha_m)\\ &= [b_1(\alpha_m)\xi + b_3(\alpha_m)\xi^3] + \dot{\xi}[b_0 + b_2(\alpha_m) + b_4(\alpha_m)\xi^2]\\ &= F_0(\xi;\alpha_m) + \dot{\xi}F_1(\xi;\alpha_m)\end{aligned} \tag{42}$$

Taking account of the scaling factors adopted in Ref. 19,

$$b_i(\alpha_m) = \kappa^2 C_1 a_i(\alpha_m), \quad (i = 1, 3) \tag{43a}$$

$$b_j(\alpha_m) = \kappa C_1 a_j(\alpha_m), \quad (j = 2, 4) \tag{43b}$$

In Eqs. (43), κ is a factor accounting for the difference between scalings adopted for the time variable in Ref. 19 and this study. From Ref. 19, $\kappa = 2c/L = 2 \times 0.429/0.107 = 8$, $C_1 = 0.088$. The $a_i(\alpha_m)$ are tabulated in Table 5 of Ref. 19, which yields the following table for the $b_i(\alpha_m)$:

α_m	10°	15°	20°	25°
b_1	-0.0265	-0.0721	-0.1977	-0.3320
b_2	-0.0101	0.0090	0.0596	0.0959
b_3	-0.1222	-0.2714	-0.0501	0.2894
b_4	+0.1491	0.1159	-0.1799	-0.9977

From Eq. (11b), the linear contribution to the damping in roll is

$$D(\alpha_m) = -F_1(0;\alpha_m) = -b_0 - b_2(\alpha_m) \tag{44}$$

where $-b_0 > 0$ is proportional to the wind-off roll-damping moment due to bearing friction in the experimental setup used in Ref. 18. In order to compare our theoretical prediction with the experimental results of Ref. 18, we choose a value of $-b_0$ such that Eq. (44) yields zero damping in roll at the same angle of attack, $\alpha_{cr} = 18.6°$, as that reported in Ref. 18. The function $D(\alpha_m)$ is then plotted in Fig. 7 by means of spline fitting.

From Eq. (26c), the index for stability of the bifurcation periodic rolling oscillation is

$$\mu = -\frac{\varepsilon^2\omega_0}{2}\frac{b_4(\alpha_{cr})}{b_1(\alpha_{cr})} \tag{45}$$

At $\alpha_{cr} = 18.6°$, we find from the table above that $b_1(\alpha_{cr}) = -0.1591 < 0$. From the spline-fit curve for $b_4(\alpha_{cr})$ (Fig. 8), we find that $b_4(\alpha_{cr}) = -0.05473$. Hence $\mu < 0$ and the bifurcation is supercritical, implying that the bifurcation periodic roll oscillation is stable. This is in agreement with the experimental finding in Ref. 18.

We now further compare the supercritical bifurcation diagram predicted by the present theory with experimental results from Ref. 18. Combining Eq. (21c) with Eq. (22) to eliminate λ_2 and then using Eq. (45), we get

$$\alpha_m - \alpha_{cr} = -\varepsilon^2 \left[\frac{\omega_0}{2} \frac{b_4}{D' b_1}\right]_{\alpha_m=\alpha_{cr}}$$

$$= \varepsilon^2 \left[\frac{b_4}{2D'\sqrt{-b_1}}\right]_{\alpha_m=\alpha_{cr}} \tag{46}$$

The last equation was obtained by using Eqs. (25) and (42). From Fig. 7 (noting that $1^\circ = \pi/180$), we get $D'(\alpha_{cr}) = -0.6131$. Hence Eq. (46) reduces to

$$\alpha_m - \alpha_{cr} = 0.1120\ \varepsilon^2 \tag{47}$$

where ε is the amplitude of the bifurcation periodic solution (Ref. 11). Equation (47) is plotted in Fig. 9 for the 80° sweep-back delta wing and compared with the experimental results of Levin and Katz (Ref. 18). The agreement is excellent near α_{cr}, where the bifurcation theory is particularly applicable.

It should be noted that although $\mu < 0$ and the bifurcation is supercritical, the magnitude of $|\mu|$ is small in the example. This implies that the bifurcation is close to the boundary between subcritical and supercritical. Consequently, on increasing the angle of attack α_m by a small amount, the amplitude of the resulting periodic motion will be quite large. This is confirmed by the experimental results shown in Fig. 9. For example, increasing α_m by 1° past α_{cr} (=18.6°) results in a stable periodic roll oscillation with an amplitude of 22.6°.

5. CONCLUDING REMARKS

We have shown how bifurcation theory can be used to study the nonlinear dynamic stability characteristics of an aircraft or flap subject to single-degree-of-freedom motion about its trim position. When the bifurcation parameter λ (e.g., the angle of attack) is increased past the stability boundary λ_{cr}, where the aerodynamic damping vanishes, the steady motion loses its stability. This results in a finite-amplitude periodic motion after the transient motion has died away. We have also established a simple criterion for the stability of the bifurcation periodic motion in terms of the aerodynamic coefficients. The theory predicts that bifurcation solutions are unstable (subcritical) for the pitching airfoil in supersonic/hypersonic flow and for flap oscillations in transonic flow. Bifurcation solutions are stable (supercritical) for roll oscillations of the slender delta wing in subsonic flow. The latter prediction is in good agreement with available experimental results.

When the theory predicts subcritical bifurcation, the abrupt change in the motion that results when λ is increased past λ_{cr} may cause an abrupt structural change of the flow field. This in turn may render invalid the form of the perturbation moment of the aerodynamic forces that was used. Under these conditions, aerodynamic information in a different form may be required. However, the theory as developed in this paper is valid up to λ_{cr} and can be used to predict the onset of subcritical bifurcation.

When the theory predicts supercritical bifurcation, the bifurcation periodic solution is stable to small disturbances for a range of λ beyond λ_{cr}. With further increase in λ, however, the periodic motion may lose its stability. This in turn may result in another bifurcation at $\lambda = \lambda_2 > \lambda_{cr}$, which could be either subcritical or supercritical. The resulting bifurcation solution may be quasi-periodic, and the sequence of bifurcations may continue.

Finally, the theory may be generalized to apply to aircraft motions involving more than a single degree of freedom. For motions involving two degrees of freedom or more, one should be aware of the possibility of chaotic behavior occurring after a finite number of successive bifurcations.

REFERENCES

1. Orlik-Rückemann, K. J., "Dynamic Stability Testing of Aircraft--Needs Versus Capabilities." Progress in Aerospace Sciences, Vol. 16, No. 4, Pergamon Press, New York, pp. 431-447, 1975.

2. Padfield, G. D., "Nonlinear Oscillations at High Incidence." AGARD CP-235, Dynamic Stability Parameters, Paper No. 31, May 1978.

3. Iooss, G. and Joseph, D. D., "Elementary Stability and Bifurcation Theory," Springer-Verlag, New York, 1980.

4. Mehra, R. K. and Carroll, J. V., "Bifurcation Analysis of Aircraft High Angle of Attack Flight Dynamics," New Approaches to Nonlinear Problems in Dynamics, Ed. P. J. Holmes, SIAM, Philadelphia, 1980, pp. 127-146.

5. Guicheteau, P., "Bifurcation Theory Applied to the Study of Control Losses on Combat Aircraft," La Recherche Aerospatiale, 1982-83, pp. 1-14.

6. Hui, W. H., "Stability of Oscillating Wedges and Caret Wings in Hypersonic and Supersonic Flows," AIAA J., Vol. 7, No. 8, Aug. 1969, pp. 1524-1530.

7. Hui, W. H., "Supersonic/Hypersonic Flow Past an Oscillating Flat-Plate at High Angles of Attack," ZAMP, Vol. 29, Fasc. 3, 1978, pp. 414-427.

8. Hui, W. H., "An Analytic Theory of Supersonic/Hypersonic Stability at High Angles of Attack," AGARD CP-235, Dynamic Stability Parameters, Paper No. 22, May 1978.

9. Hui, W. H. and Tobak, M., "Unsteady Newton-Busemann Flow Theory. Part I: Airfoils," AIAA J., Vol. 19, No. 3, Mar. 1981, pp. 311-318.

10. Hui, W. H., "Large-Amplitude Slow Oscillation of Wedges in Inviscid Hypersonic and Supersonic Flows," AIAA J., Vol. 8, No. 8, Aug. 1970, pp. 1530-1532.

11. Hui, W. H. and Tobak, M., "Bifurcation Analysis of Aircraft Pitching Motions About Large Mean Angles of Attack," J. Guidance, Control, and Dynamics, Vol. 7, 1984, pp. 113-122.

12. Chyu, W. J. and Schiff, L. B., "Nonlinear Aerodynamic Modeling of Flap Oscillations in Transonic Flow: A Numerical Validation," AIAA J., Vol. 21, No. 1, Jan. 1983, pp. 106-113.

13. Nguyen, L. T., Yip, L., and Chambers, J. R., "Self-Induced Wing Rock of Slender Delta Wings," AIAA Paper 81-1883, Atmospheric Flight Mechanics Conference, Albuquerque, NM, Aug. 1981.

14. Tobak, M. and Schiff, L. B., "Aerodynamic Mathematical Modeling--Basic Concepts," AGARD Lecture Series No. 114 on Dynamic Stability Parameters, Lecture No. 1, March 1981.

15. Hopf, E., "Abzweigung einer periodischen Lösung von einer Stationären Lösung einer Differentialsystems," Berichten der Mathematisch-Physischen Klasse der Sächsischen Akademie der Wissenschaften zu Leipzig, Vol. XCIV, 1942, pp. 1-22.

16. Hui, W. H., "Unified Unsteady Supersonic/Hypersonic Theory of Flow Past Double Wedge Aerofoils," ZAMP, Vol. 34, 1983, pp. 458-488.

17. Tobak, M. and Schiff, L. B., "On the Formulation of the Aerodynamic Characteristics in Aircraft Dynamics," NASA TR R-456, Jan. 1976.

18. Levin, D. and Katz, J., "Dynamic Load Measurements with Delta Wings Undergoing Self-Induced Roll-Oscillations," J. Aircraft, Vol. 21, 1984, pp. 30-36.

19. Konstadinopoulos, K., Mook, D. T., and Nayfeh, A. H., "Subsonic Wing Rock of Slender Delta Wing," AIAA Paper 85-0198, Jan. 1985.

20. Hsu, C. H. and Lan, C. E., "Theory of Wing Rock," AIAA Paper 85-0199, Jan. 1985.

21. Ericsson, L. E., "The Fluid Mechanics of Slender Wing Rock," J. Aircraft, Vol. 21, 1984, pp. 322-328.

ACKNOWLEDGMENT

Professor Hui's contributions to this study were funded by NASA Grant NAGW-575.

TABLE 1. VALUES OF STABILITY CRITERION $\mu(M_\infty, h)$ FOR FLAT-PLATE AIRFOIL; $\varepsilon = 1$, $\gamma = 1.4$; $\mu > 0$ SUBCRITICAL BIFURCATION, $\mu < 0$ SUPERCRITICAL BIFURCATION

M_∞ \ h	0	0.1	0.2	0.3	0.4	M_∞ \ h	0	0.1	0.2	0.3	0.4
1.5	36.5	19.0	---	---	---	2	39.5	25.8	17.2	13.0	14.7
1.6	39.6	23.4	13.6	8.8	10.7	3	57.2	38.6	26.8	20.9	23.3
1.7	40.0	24.8	15.5	11.0	12.8	4	84.7	58.4	41.4	32.8	36.4
1.8	39.7	25.3	16.3	12.0	13.7	5	107.3	74.8	53.7	42.9	47.5
1.9	39.4	25.5	16.8	12.6	14.3	6	123.6	86.7	62.6	50.3	55.6
2.0	39.5	25.8	17.2	13.0	14.7						

M_∞ \ h	0.25	0.26	0.27	0.28	0.29	0.30	0.31	0.32	0.33	0.34	0.35
1.6	10.6	10.1	9.7	9.3	9.0	8.8	8.6	8.5	8.4	8.4	8.5
1.7	12.6	12.2	11.8	11.5	11.2	11.0	10.8	10.7	10.6	10.6	10.7
1.8	13.6	13.2	12.8	12.5	12.2	12.0	11.8	11.7	11.6	11.7	11.7
1.9	14.1	13.7	13.4	13.0	12.8	12.5	12.4	12.3	12.2	12.2	12.3
2.0	14.5	14.1	13.8	13.5	13.2	13.0	12.8	12.7	12.6	12.7	12.7

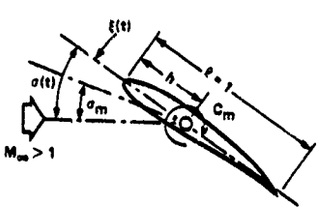

Fig. 1. Pitching airfoil in supersonic/hypersonic flow.

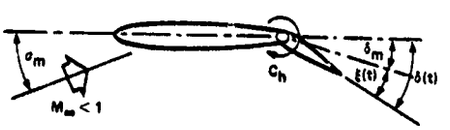

Fig. 2. Flap oscillation in transonic flow.

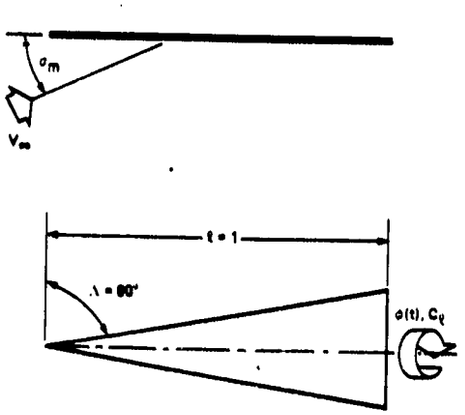

Fig. 3. Wing rock of slender delta wing in subsonic flow.

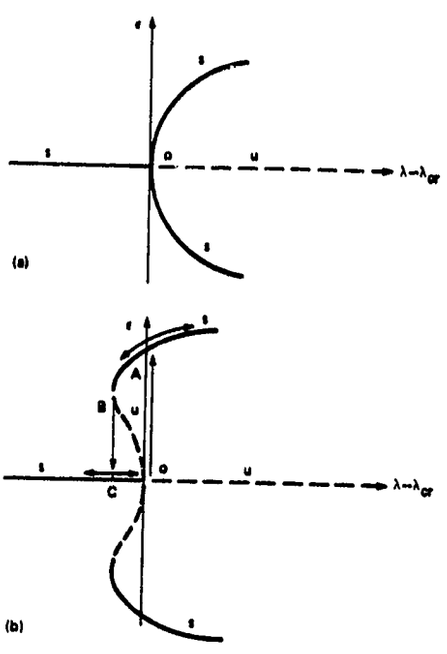

Fig. 4. Typical forms of bifurcation diagrams near the dynamic stability boundary λ_{cr} where $D(\lambda_{cr}) = 0$. (a) Supercritical, $\mu < 0$. (b) Subcritical, $\mu > 0$.

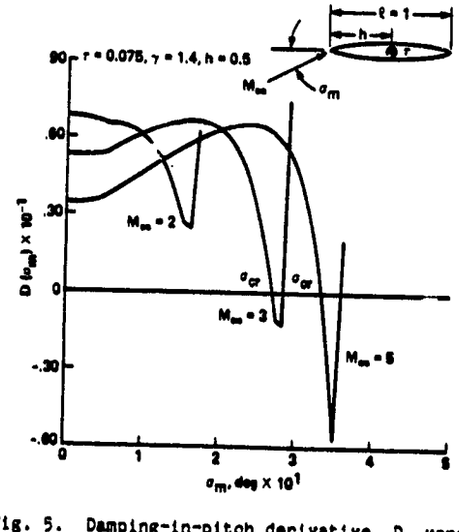

Fig. 5. Damping-in-pitch derivative D versus angle of attack σ_m for a biconvex circular arc airfoil (Ref. 16), h = 0.5, γ = 1.4, τ = 0.075.

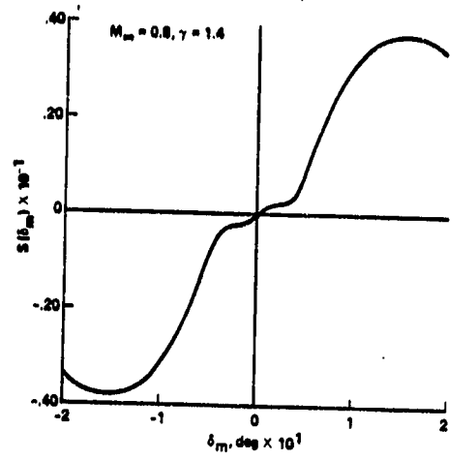

Fig. 6a. Stiffness derivative S versus mean deflection angle δ_m of a transonic flap on NASA 64A010 airfoil (Ref. 12). $M_\infty = 0.8$, $\gamma = 1.4$, $\sigma_m = 0$.

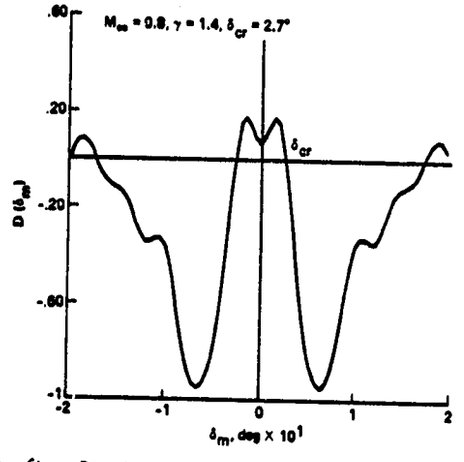

Fig. 6b. Damping derivative D versus mean deflection angle δ_m of a transonic flap on NASA 64A010 airfoil (Ref. 12). $M_\infty = 0.8$, $\gamma = 1.4$, $\sigma_m = 0$, $\delta_{cr} = 2.7°$.

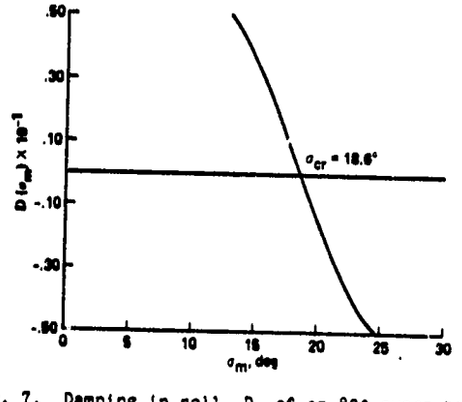

Fig. 7. Damping in roll D of an 80° sweep-back flat delta wing versus angle of attack σ_m in incompressible flow (Refs. 18, 19), Eq. (44). $\sigma_{cr} = 18.6°$.

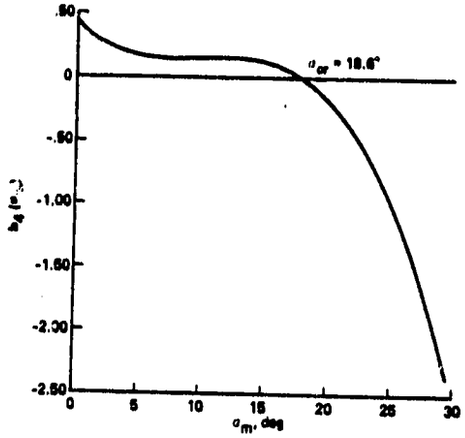

Fig. 8. Rolling aerodynamic coefficient $b_4(\alpha_m)$ of an 80° sweep-back flat delta wing versus angle of attack α_m in incompressible flow (Refs. 18, 19). Observe $b_4(\alpha_{cr}) = -0.05473 < 0$.

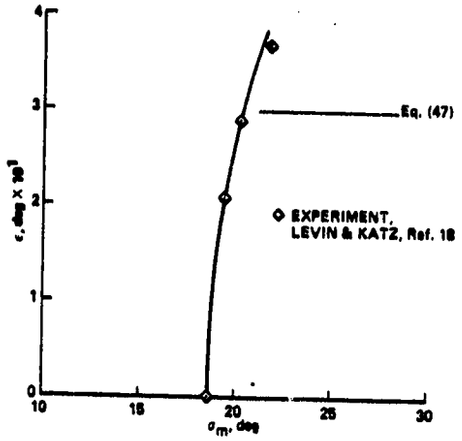

Fig. 9. Amplitude ε of bifurcation periodic motion of an 80° sweep-back delta wing versus angle of attack α_m; Eq. (47); ◇ experiments (Ref. 18). $\alpha_{cr} = 18.6°$.